Thermo-mechanical loading of GFRP reinforced thin concrete panels

Andreas Schmitt [a], Valter Carvelli [b, *], Matthias Pahn [a]

[a] Fachgebiet Massivbau und Baukonstruktion, Technische Universität Kaiserslautern, Paul-Ehrlich-Straße, D-67663 Kaiserslautern, Germany
[b] Department of Architecture, Built Environment and Construction Engineering, Politecnico di Milano, Piazza Leonardo Da Vinci 32, 20133 Milan, Italy

Received 11 January 2015 Received in revised form 21 May 2015
Accepted 29 June 2015 Available online 8 July 2015

1. Introduction

The possibility in replacing steel rebars with GFRP (Glass Fibre Reinforced Polymer) rebars in reinforced concrete was increasingly investigated in the last decades [1]. The main advantages in using GFRP reinforcement are: their lightweight nature for weight sensitive structures, their non-corrosive and non-conductive characteristics, as well as their high strength-to-weight ratio [2]. Recently, efforts were dedicated in improving the service life of GFRP reinforced concrete structural elements exposed to severe environmental conditions ([3,4]). The potential advantages of composite rebars were already demonstrated, but some aspects concerning the durability or the reaction to elevated temperatures are still topics of investigation. In particular, GFRP presents poor resistance to elevated temperature due to the low value of the glass transition temperature of the polymeric matrix. It can be in the range of 80–180 °C. A temperature of this level could be easily overcome during fire exposure. Exceeding the transition temperature causes reduction in adhesion to concrete, in stiffness and strength of the rebars, which have to be considered for the design of a reinforced concrete structure.

Some investigations were published for understanding the thermo-mechanical behaviour of structural concrete beams and slabs internally reinforced with FRP bars. The strength and deformability of GFRP reinforced concrete slabs in fire situations were detailed in Refs. [5] and [6]. The authors underlined the importance of the concrete cover and of the bars anchorage length as fundamental parameters for the fire resistance of concrete members. In Ref. [7], concrete slabs reinforced by GFRP rebars were tested with emphasis on their ability to sustain loads under fire exposure. Another experimental campaign on concrete members reinforced with GFRP bars exposed to temperature above 500 °C on a portion of the external surface is detailed in Ref. [8]. In this research, the influence of the reinforcement geometry on the load carrying capacity was investigated. The behaviour of GFRP reinforced concrete beams exposed to fire was also discussed in Ref. [9]. The degradation of the flexural capacity due to fire was evaluated and the agreement with the fire design requirements, for the minimum periods of fire resistance, was assessed assuming a minimum concrete cover.

Beside the experimental investigations, some researches were dedicated to the numerical and analytical modelling of the performance under high temperature conditions of structural concrete members reinforced with FRP bars. Methods estimating the residual flexural and shear strengths of reinforced beams exposed to fire are detailed in Ref. [10]. The proposed methods consider the reduction of the initial strengths of concrete and FRP reinforcement resulting from the high temperatures developed inside the beam.

The adhesion between the FRP bar and concrete can be extensively compromised at elevated temperature [11]. A bond model taking temperature effects into account was proposed in Ref. [12]. It predicts the necessary anchoring length in the protected zones

* Corresponding author. Tel.: +39 0223994354.
E-mail address: valter.carvelli@polimi.it (V. Carvelli).

(cold anchorage). More refined and accurate predictions were obtained with numerical finite element models (see e.g. Refs. [13,14]). These can account for the properties of materials at high temperatures, realistic load and boundary conditions, as well as temperature induced slip between FRP rebars and concrete.

Based on the continuous research in the last decades, some guidelines and codes were proposed, but only the Canadian code [15] provides a design procedure for structural concrete members in fire situations, in the authors' knowledge. Recently, in Ref. [16] a simplified design method (for both thermal and mechanical analyses) was proposed to estimate the bending moment resistance of FRP reinforced concrete slabs in fire situations.

The above mentioned and other researches available in the literature are dedicated to FRP reinforced concrete members with bearing function. But in construction engineering several low bearing function concrete components have a relevant importance. In particular, very thin concrete elements are adopted like façade panels or slabs for pavements.

External cladding panels made of pre-cast concrete usually consist of three layers: the load carrying concrete layer, the thermal insulation and a thin facing concrete layer. Such panels are an economic and energy-efficient alternative to the usual in-situ concrete construction. Recently, the non-corrosive GFRP bars were adopted as reinforcement for the facing concrete layer of slender sandwich wall panels to reduce the concrete cover and simultaneously the thickness of the concrete layers (see e.g. Refs. [17,18]). Moreover, the low bearing capacity of such reinforced concrete layer allows to minimize the thickness and, as consequence, to reduce the total weight of the panels.

In spite of the interest in constructions industry on low bearing function FRP reinforced concrete members, their durability and in particular their thermo-mechanical behaviour is not deeply known and investigated, in the authors' knowledge. The latter is very important in external cladding of buildings or in pavements exposed to irradiation in very warm climates.

In this paper, an experimental investigation is detailed aiming in understanding the behaviour of thin concrete panels reinforced with GFRP rebars exposed to increasing temperature and bending loading. The considered thin panels (thickness of 4 cm) are typical for low bearing function concrete layers in façade claddings. The influence of two aspects was studied: the concrete cover and the external surface of rebars.

The adopted heating condition allowed to have the temperature of the internal GFRP rebars almost at the level of the transition temperature of the resin. This does not match to a real fire exposure, but to an extreme heating condition of low bearing panels. The consequences of this extreme condition were assessed measuring the variation of the deformability and of the load carrying capacity of the panels with post-heating bending tests. The thin concrete panels, exposed to a temperature higher than expected in real applications, had an excellent mechanical response. The elevated temperature did not produce degradation of the rebars and of the rebar-concrete adhesion. A relevant consequence of the loading and heating was the reduction of the initial global stiffness due to the imparted cracking patterns.

2. Materials and samples

The geometry of the specimens (170 × 40 × 4 cm) is detailed in Fig. 1. The length and the width are the maximum for the available heating device.

Two concrete covers were considered, 5 and 10 mm and two GFRP unidirectional E-glass rebars, named commercially: Schöck ComBAR® and FiReP® Rebar P ([19,20]), in the following B1 and B2, respectively.

The considered concrete panels do not have shear reinforcement.

The number of tests for each combination of rebar and concrete cover is summarized in Table 1. The limited number of tests is not statistically significant but, however, they provide a clear understanding of the thermo-mechanical behaviour under the considered conditions.

The GFRP rebars were produced by pultrusion technique. Depending upon the producer, a variety of diameters and surface conditions are available in the market. ComBAR® has external ribbed surface, cut into the bar after curing (Fig. 2a). The eternal surface of FiReP® Rebar P is produced with a wave shaped thread profile during pultrusion (Fig. 2b).

For both rebars, vinyl ester resins were adopted with glass transition temperature of about 180 °C, according to the producers.

The nominal diameter of the adopted rebars is 8 mm. According to the data sheet of the producers, the mechanical properties of the rebars are very similar ([19,20]). In the direction of the bar axis, the tensile strength is ≈1000 MPa and the elastic modulus is ≈60 GPa.

Table 1
Number of tests.

		Concrete cover	
		5 mm	10 mm
Rebar ∅8 mm	Schöck ComBAR®	2	2
	FiReP® Rebar P	2	2

Fig. 1. Specimen geometry and reinforcement.

(a) (b)

Fig. 2. Rebars external surface: (a) Schöck ComBAR®; (b) FiReP® Rebar P.

The specimens were casted in movable formworks, to enable an appropriate compaction of the concrete with an external vibrator.

The concrete mix contains for m^3: 187 kg of water; 450 kg of cement CEM 42.5 N; 525 kg of aggregates 0/2 mm; 580 kg of aggregates 2/8 mm; 530 kg of aggregates 8/16 mm; 1.37 kg of liquefier.

During casting, some specimens were prepared to measure the mechanical properties of the concrete at room temperature. The compressive tests provided average (of three specimens) cubic strength of 61.9 MPa and compressive elastic modulus of 28 GPa. Three cylinders were adopted to measure the tensile strength of the concrete. The indirect tensile tests [21] gave an average tensile strength of 3.5 MPa. Accordingly, the concrete was of quality C45/55.

3. Experimental setup and procedure

The response of GFRP reinforced concrete panels was investigated with two consecutive experimental phases. In the first phase, a bending constant load was applied and then the panel was heated up to the considered maximum temperature, while in the second phase the post-heating mechanical response was measured under bending loading up to failure at room temperature.

3.1. First phase: thermo-mechanical loading

In the first phase, a quasi-static four-points bending loading was imposed with supports span of $L = 140$ cm and loads span of 50 cm (see Fig. 3). The cylindrical supports (diameter 50 mm) were set on the heating device to have the concrete panel as top side closure (Fig. 4). At the maximum imposed load, the heating started increasing the temperature on the full bottom surface of the specimen.

The bending loading was applied quasi-statically increasing the dead load in almost 2 min up to the maximum resultant of 3.6 kN (specimen own weight is not included) to impart a low level of damage before heating. The maximum load was estimated, by ACI-440 [22], in the range of the theoretical concrete first cracking, that is supposed to start at about 2.6 kN (Fig. 5). Once the maximum load was reached, it remained constant for the heating time.

The heating on the bottom surface of the specimen was applied by the device in Fig. 4a. This is an electronically controlled oven

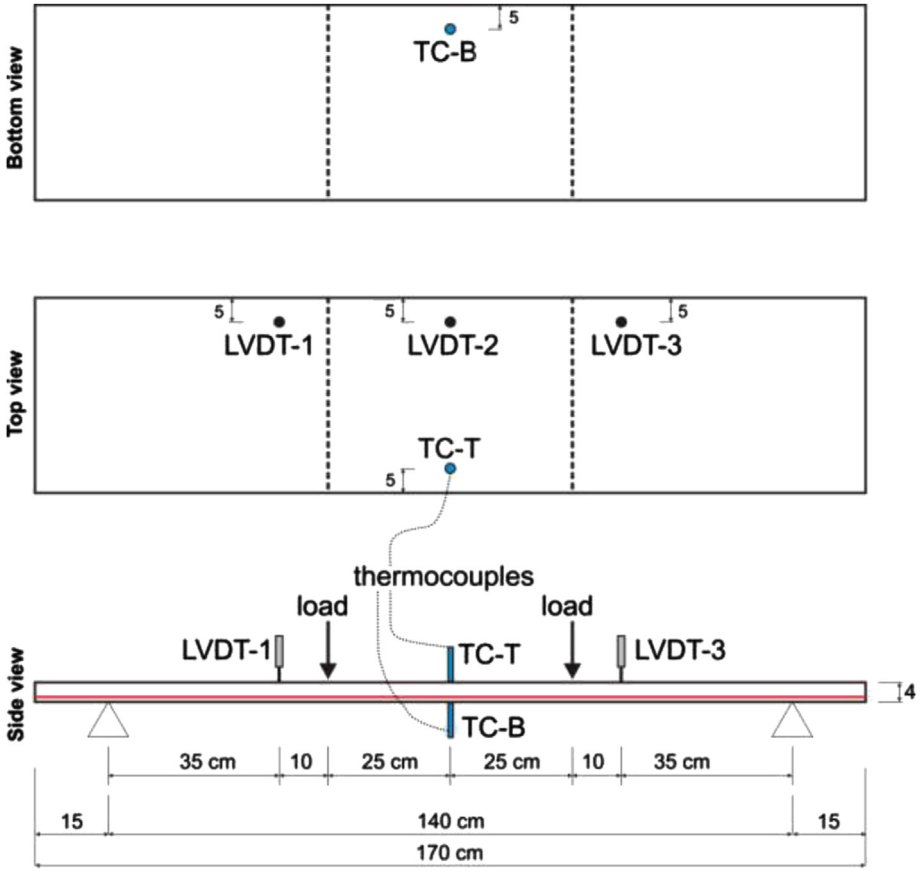

Fig. 3. Test set-up: scheme of some instruments position.

(a)

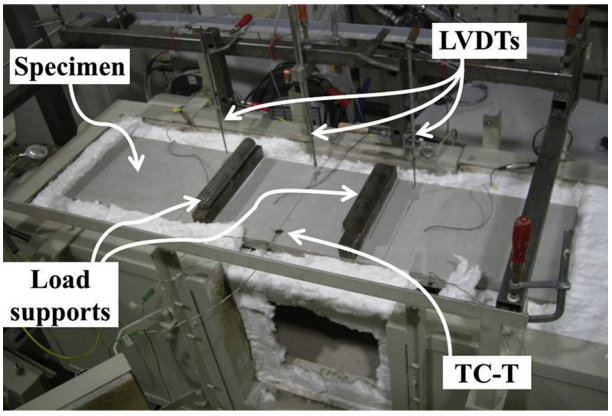

(b)

Fig. 4. Test set-up: (a) heating device; (b) specimens and some instruments position.

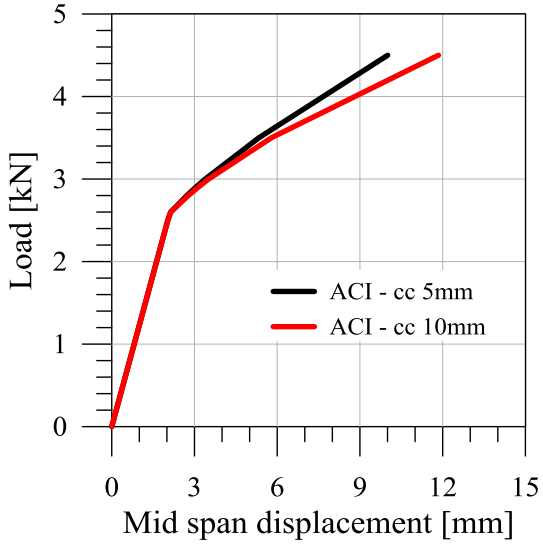

Fig. 5. Load vs. mid span displacement prediction by ACI-440 for the initial load stage.

with maximum temperature of more than 1000 °C. The heating is generated by a gas burner and the temperature is controlled by a thermocouple in the centre of the device. To avoid the direct contact of the flame on the bottom surface of the specimen, a layer of insulating material (4 cm thick) was mounted at the mid height of the oven. This allowed the flame to remain on the bottom part of the oven chamber and the hot air to flow on the top part, where the specimen was uniformly heated.

The temperature on the bottom and top surface of the specimen was continuously measured by two thermocouples (TC-B and TC-T) in the mid span at 5 cm from one longitudinal side (see Fig. 3).

The heating of the device was controlled considering the temperature on the bottom surface of the specimen with TC-B.

After the application of the bending load, the temperature on the bottom surface of the specimen was increased from the room temperature (25 °C) to the maximum of 210 °C. When the temperature of the bottom surface reached the desired maximum, it was maintained nearly constant for about 65 min.

The maximum imposed temperature is not such as in some real applications of thin concrete panels (e.g. on façade panels the temperature could be below 100 °C in very warm latitudes). It was considered to investigate the thermo-mechanic behaviour under an extreme condition. The maximum temperature of 210 °C was imposed to reach at the rebars level almost the glass transition temperature of the adopted resins ($T_g \approx 180$ °C) (see Section 2). The diagrams in Fig. 7 show two representative evolutions in time of the temperature recorded on the bottom and top surface of specimens with the two concrete covers. The maximum recorded temperature on the top surface was about 120 °C, after 65 min of exposition. Assuming a linear distribution of the temperature in the thickness of the specimen (this is reasonable for the considered small thickness), at the bar level the temperature should be about 189 °C and 178 °C for 5 and 10 mm cover, respectively.

During loading and heating, the deflection of the specimen was measured by three transducers (LVDT), one in the mid span and two 35 cm beside both supports (see Figs. 3 and 4b). They were placed on the top surface, 5 cm away from a longitudinal side.

Moreover, three strain gauges were glued on the bottom of the central rebar, to monitor the longitudinal deformation of one bar at the interface with concrete. The sketch in Fig. 6 details the position of the strain gauges. Unfortunately, a modification of the electrical signal, only during heating of the oven, did not provide the correct measurement of the strain when the temperature was increased and maintained constant. But, the proper recording of the strain gauges signals gave interesting information on the pre- and post-heating strain and stress level inside the panels, i.e. during the application of the load in the first phase and during the complete second phase.

3.2. Second phase: post-heating mechanical response

In the second experimental phase, the specimens were quasi-statically loaded using the same four-points bending scheme (see Fig. 3) at room temperature (see Fig. 8). This allowed comparing the mechanical behaviour of the panels after the thermo-mechanical conditioning. The same measuring instruments were adopted as in the first phase (one LVDT in the mid span of the top surface and three strain gauges on the central rebar inside the panels, see Figs. 3 and 6), and a jack with a load cell of 50 kN.

4. Results and discussion

4.1. First phase

In the first experimental phase the thermo-mechanical loading was subdivided in three consecutive steps (see Fig. 7):

1 Mechanical loading up to the considered maximum load (3.6 kN);

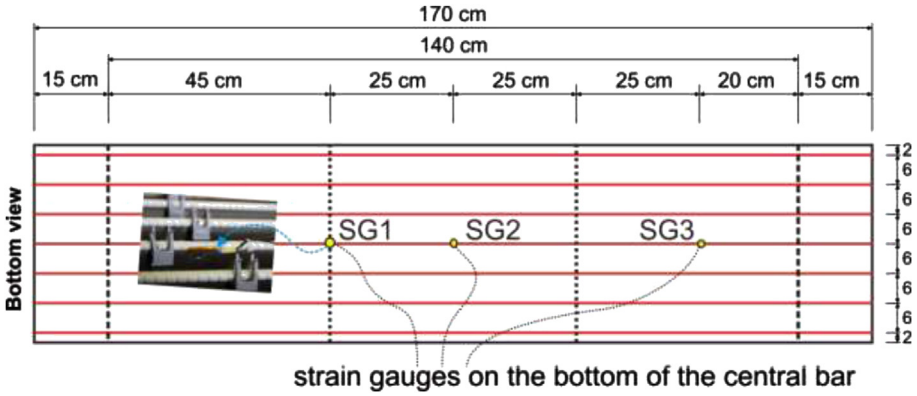

Fig. 6. Test set-up: scheme of strain gauges position.

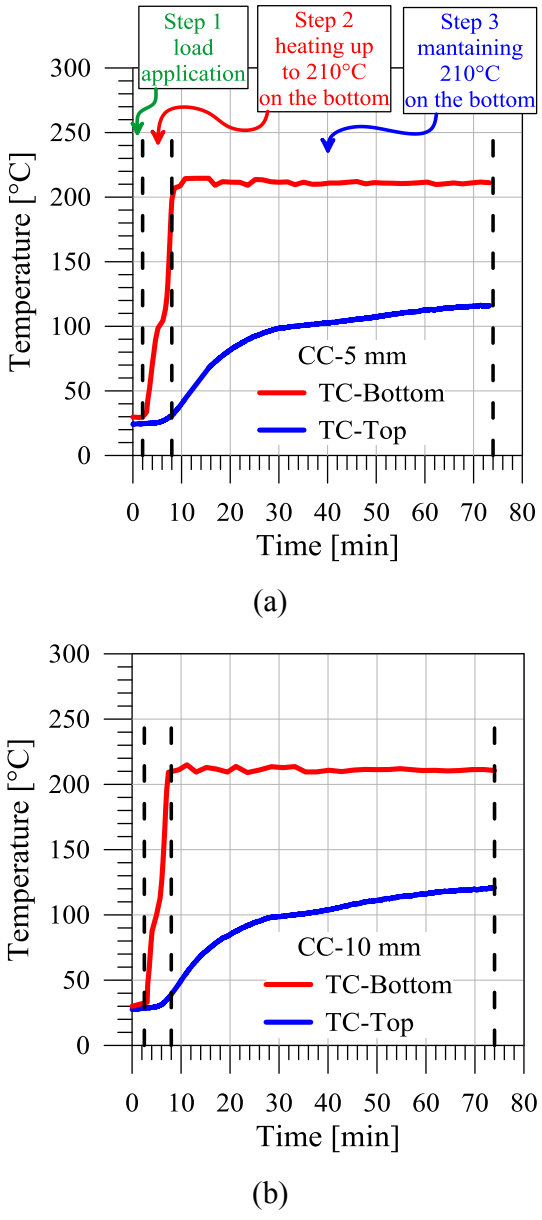

Fig. 7. Representative diagrams temperature vs. time of specimens reinforced with Schöck ComBAR® for (a) 5 mm and (b) 10 mm concrete cover.

Fig. 8. Post-heating four points bending test at room temperature.

2 Heating up to the maximum considered temperature (210 °C) on the bottom;
3 Maintaining the temperature constant on the bottom surface for 65 min.

During these steps, the continuous recording of the LVDTs provided the evolution of the displacement as illustrated in Fig. 9. The measurements of the three LVDTs, on specimens reinforced with ComBAR® (see Fig. 9), show the influence of the three steps on the global deformation. In particular, in the first step (bending loading) the mid span displacement (LVDT2) of the panels with concrete cover 5 mm was lower, as expected, than that of panels with 10 mm cover. The heating in the second step generated an increase of mid span displacement, with respect to the first step, of almost 45% and 25% for concrete cover of 5 and 10 mm, respectively. The diffusion of the temperature in the third step raised the displacement in the centre of about 16% and 24%. The contributions on the mid span displacement of the three steps are compared in Fig. 10 for the two bars and two concrete covers. On one hand, as observed above, the smallest concrete cover resulted in the lowest deflection for both rebars. On the other, the influence of the rebar external surface was visible; the panels with ComBAR® rebars had the lowest mid span displacement for both concrete covers and in each step of the thermo-mechanical loading. The residual average deflection after unloading and complete cooling (step 4 in Fig. 10) was about 9 mm and 11 mm for 5 mm and 10 mm concrete cover, respectively, with a difference of almost 1 mm between the two rebars.

The strains on the central bars are collected in Fig. 11. These values were measured by the three strain gauges after the application of the maximum load, before the heating was started. As observed above, the panels with the highest concrete cover had

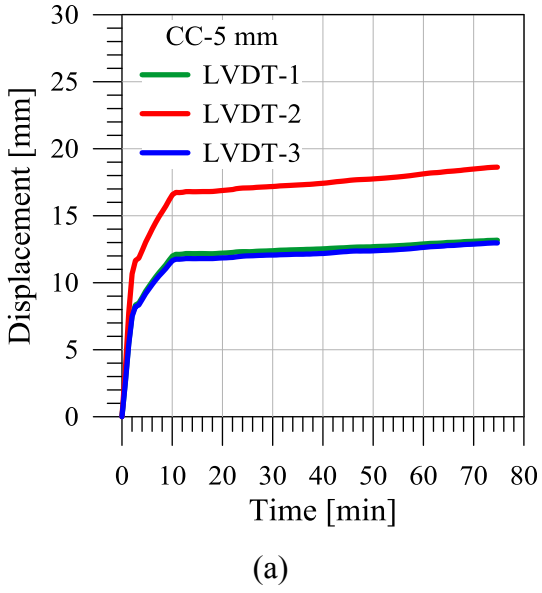

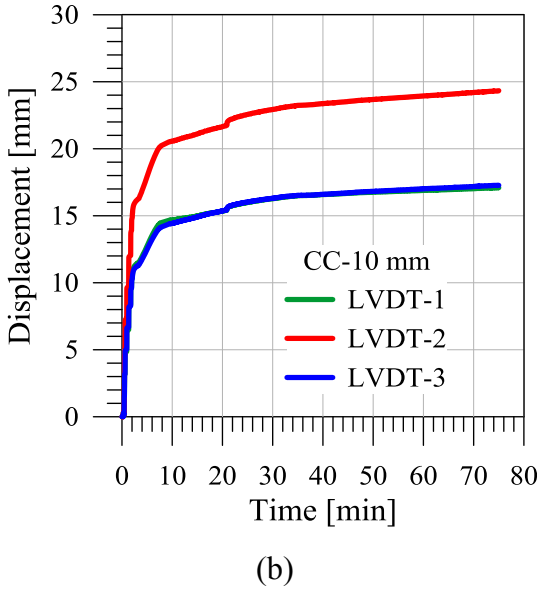

Fig. 9. Representative diagrams LVDTs displacement vs. time of specimens reinforced with Schöck ComBAR® for (a) 5 mm and (b) 10 mm concrete cover. 'cc' means concrete cover.

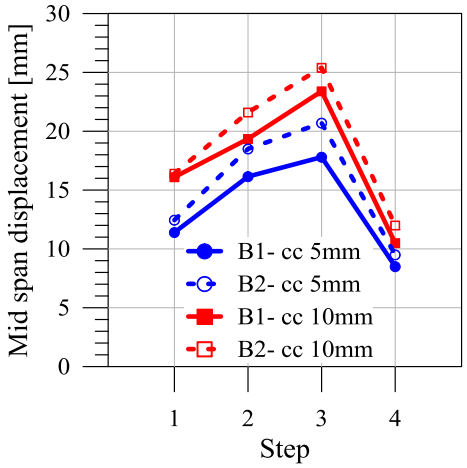

Fig. 10. Average LVDT mid span displacement at different steps: 1 at the maximum load before heating; 2 after heating up; 3 after 65 min of maintaining the maximum temperature; 4 after unloading and complete cooling. B1 and B2 indicate Schöck ComBAR® and FiReP® Rebar P, respectively. 'cc' means concrete cover.

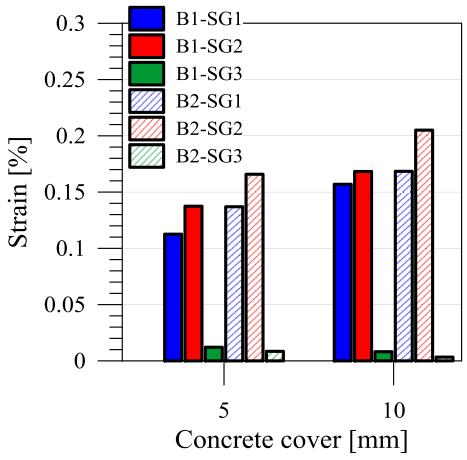

Fig. 11. Average strain of the three strain gauges at the maximum load before heating. B1 and B2 indicate Schöck ComBAR® and FiReP® Rebar P, respectively.

Table 2
Estimation of the stress level in the rebars (values in MPa) at the maximum load before heating.

	Concrete cover	
	5 mm	10 mm
Schöck ComBAR®	82	101
FiReP® Rebar P	100	123

the highest global deformation; this is reflected in the strain measurements. The strain in the mid span (SG2) of the specimens with concrete cover 10 mm was about 23% higher than the strain of the specimens with 5 mm cover, for both rebars. The influence of the external surface of the two rebars is also visible comparing the strains. The average strain of the FiReP® rebar was about 21% higher than the strain of the ComBAR®, for both concrete covers. The strains allow estimating the stress in the bar at the considered load level, assuming a linear elastic behaviour of the bar material and an elastic modulus of 60 GPa, as in the data sheet of the producers. The average stresses in the rebars, for the maximum bending load before heating, are listed in Table 2. The stress level of the rebars was almost one tenth of their strength.

The thermo-mechanical loading of the first experimental phase developed the cracks patterns on the bottom surface of the panels in Fig. 12, where the longest cracks were highlighted. The main distribution of the cracks is located, as expected, in the central part of the panels between the two loads where the constant maximum bending moment was generated. The panels with different rebars and concrete covers did not show considerable differences in the crack patterns.

4.2. Second phase

The influence of coupling mechanical load and elevated temperature on the mechanical response of the panels was measured in the second experimental phase with four points bending tests up to failure at room temperature. The global response of the panels is

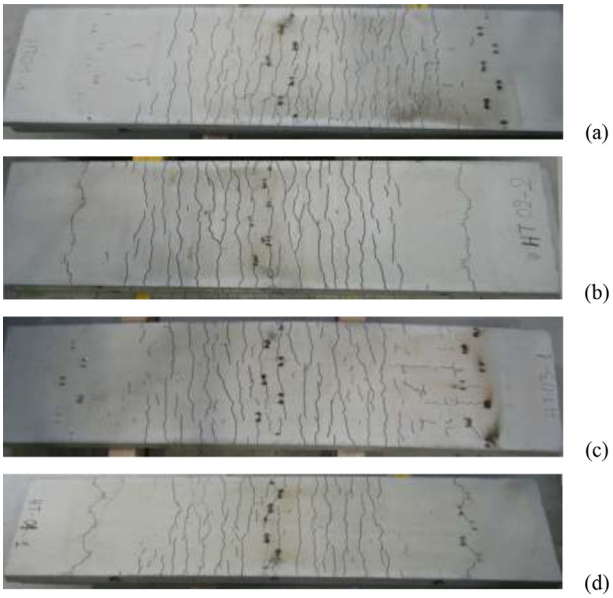

Fig. 12. Main cracks pattern after unloading and cooling. Specimens reinforced with: (a, b) Schöck ComBAR®; (c, d) FiReP® Rebar P. (a, c) 5 mm and (b, d) 10 mm concrete cover.

detailed in Fig. 13. The post-heating load vs. mid span deflection curves (Fig. 13a) show a very similar behaviour of the panels with the same concrete cover. The only relevant difference was for the failure load of the panels with 5 mm cover. The panels with ComBAR® had a maximum load almost 30% higher than those with FiReP® rebars. This is probably connected to their external surfaces leading to different adhesion failure mechanisms, more evident with the lower concrete cover.

The strain of the two different types of rebar had very similar evolution (Fig. 13b) during the post-heating bending up to the failure load of the strain gauges (lower than that of the panel). Unfortunately, the strain gauges inside panels reinforced with ComBAR® and concrete cover 10 mm did not transmit correct signals due to damaging of the cable in the heating phase. Assuming a linear elastic behaviour of the rebars, at the average failure load of the panels (≈26 kN) a rough estimation gives a stress level in the bar of about 720 MPa. This is lower than the rebar strength in the data sheet of the producers. It suggests a failure mechanism of the panel in which the rebars are not broken, as observed below.

The experimental and predicted by ACI-440 load vs. mid span displacement curves are compared in Fig. 14. In the initial load range up to the first cracking of concrete, ACI-440 [22] predicts a stiffer behaviour of the panels than the experimental results (Fig. 14a). The discrepancy could be related to the cracking imparted in the first phase, that is not included in the analytical predictions. ACI-440 and the experimental results show very similar second branch of the load-deflection curves (Fig. 14b). This highlights the accuracy of the guideline [22] in estimating the bending behaviour of such GFRP reinforced concrete panels when the influence of the rebars becomes predominant (the thermal effects are not considered in Ref. [22]).

The variation of the pre- and post-heating mechanical behaviour is detailed comparing the stiffness of the panel (global quantity) and the strain on the central rebar (local quantity) at the maximum load level of the first phase.

The initial stiffness is defined as the slope of the segment passing through the two points of a curve in Fig. 13a, at load 0.4 and 3.6 kN.

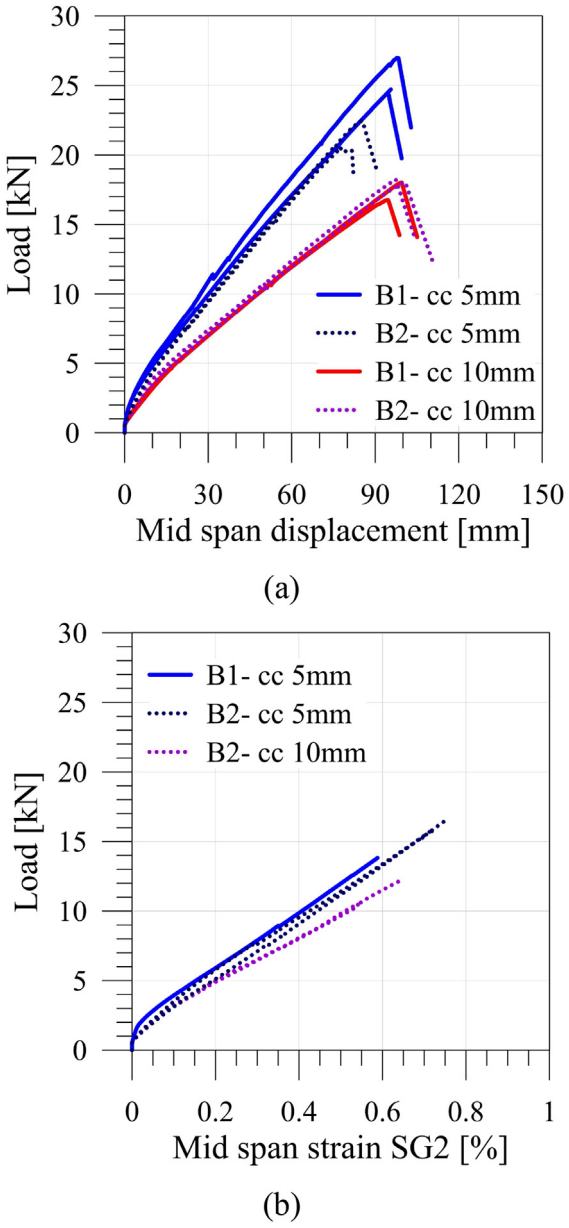

Fig. 13. Post-heating bending. Load vs. (a) LVDT mid span displacement and (b) mid span strain SG2. B1 and B2 indicate Schöck ComBAR® and FiReP® Rebar P, respectively. 'cc' means concrete cover.

The summary of the pre- and post-heating average stiffness in Fig. 15 shows the degradation of this mechanical parameter due to loading and heating. The initial stiffness of the panel had a reduction in the range 19–27%, higher for concrete cover 10 mm than 5 mm for both rebars. Moreover, the data in Fig. 15 demonstrate the effect of the bar external surface. The panels reinforced with FiReP® rebars and concrete cover of 5 mm had higher reduction of the initial stiffness than the panels with ComBAR®, while the panels with concrete cover of 10 mm had almost the same decrease of stiffness. The latter depends on the position of the bars and the involvement of the concrete on the bottom of the panel in sustaining the tensile stress.

As observed above, ACI-440 and the post-heating experimental results provide very similar second branch of the load-deflection curves (see Fig. 14b). ACI predictions do not consider the heating effects on materials. This observation and the comparison in Fig. 14

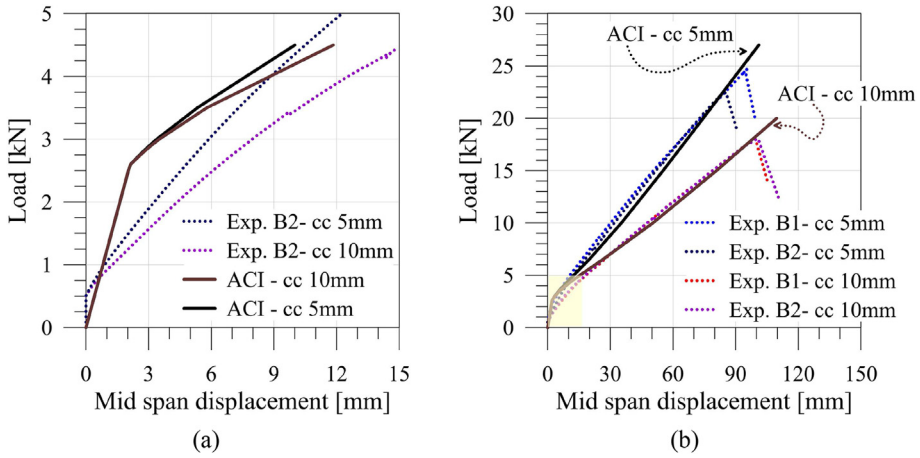

Fig. 14. Post-heating bending. Comparison of ACI-440 predictions and some experimental load vs. mid span displacement curves. (a) Comparison of the experimental results for panels with bar B2 and ACI-440 curves in the low range of load. (b) Complete curves. 'cc' means concrete cover.

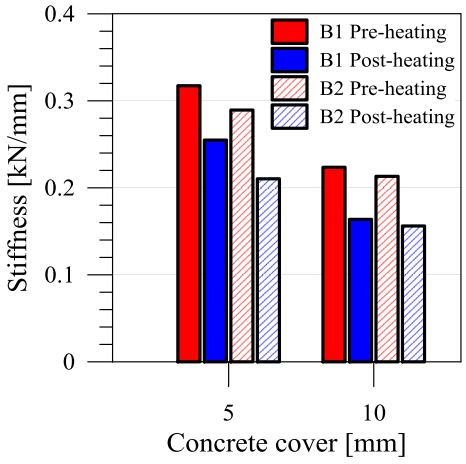

Fig. 15. Pre- and Post-heating bending. Average initial stiffness of the panels. B1 and B2 indicate Schöck ComBAR® and FiReP® Rebar P, respectively.

Fig. 16. Post-heating bending. Typical failure mode of the panels.

demonstrate a negligible effect of the imposed elevated temperature on the rebar mechanical response, and show that the reduction of the initial stiffness is mainly related to the damage in concrete.

The pre- and post-heating measurements of the strain gauges did not have a considerable variation, at the maximum load of the first stage. This suggests that the adhesion between bar and concrete was not modified by the application of the elevated temperature. This hypothesis, based on the measurements at the considered load level (which is about 14% and 20% of the average failure load of panels with 5 mm and 10 mm concrete cover), is confirmed observing the failure mode of the panels. All specimens had failure of the concrete in compression (see the typical failure mode in Fig. 16). As supposed above, the bars were not extensively damaged and not broken. Extracting some rebars from the specimens after failure, they showed still a good adhesion with concrete and an external surface not apparently modified by the elevated temperature (see Fig. 17 for rebars in panels with 5 mm concrete cover).

5. Conclusions

The experimental research was focused on understanding the thermo-mechanical response of thin concrete panels reinforced with GFRP rebars. The considered panels had 4 cm thickness and are typically adopted as low bearing function concrete components (e.g. façade panels or slabs for pavements). The influence of two aspects was investigated: the concrete cover and the external surface of rebars. The limited number of tests does not provide statistically significant results, but they give a clear trend of the panels behaviour under the considered extreme conditions. The main outcomes of the research are:

- The external surface of the GFRP rebars has considerable influence on the bending response of the panels in term of initial stiffness and local level of strain.
- Increasing the concrete cover, the initial stiffness decreases and the strain on bottom rebars increase, as expected.
- The imposed elevated temperature imparted a considerable residual deflection in the panels after complete cooling.
- The loading and heating program, in the first phase, with maximum temperature of 210 °C on the bottom, had as consequence a reduction of the initial global stiffness due to the imparted cracking patterns.
- The elevated temperature did not generate evident degradation of the GFRP reinforcement and of its adhesion to concrete.
- After heating, all specimens failed in compression of concrete, with almost intact rebars.

The obtained results demonstrate the excellent mechanical behaviour of the low bearing function thin concrete panels

(a) (b)

Fig. 17. Post-heating bending. Some rebars after failure of the panels with 5 cm concrete cover. External surface of: (a) Schöck ComBAR® and (b) FiReP® Rebar P.

reinforced with GFRP rebars exposed to a range of temperature higher than expected in real applications. These results could increase the confidence in adopting such GFRP reinforced concrete panels in environments with elevated temperature and this should be considered beside the other advantages of the GFRP bars as reinforcement in concrete.

Acknowledgements

The research was carried out in the framework of the European Cooperation in Science and Technology COST Action TU1207 – Next Generation Design Guidelines for Composites in Construction. The research was partially developed during the 'Short Term Scientific Mission' of the second Author financed by COST Action TU1207. Schöck Bauteile GmbH and FiReP Inc. are gratefully acknowledged for supplying the GFRP rebars.

References

[1] Bakis C, Bank L, Brown V, Cosenza E, Davalos J, Lesko J, et al. Fiber-reinforced polymer composites for construction — state-of-the-art review. J Compos Constr – ASCE 2002;6:73–87.
[2] GangaRao H, Taly N, Vijay P. Reinforced concrete design with FRP composites. Boca Raton, FL: CRC Press – Taylor & Francis Group; 2007.
[3] Mufti AA, Neale KW. State-of-the-art of FRP and SHM applications in bridge structures in Canada. Compos Res J 2008;2:60–9.
[4] Pendhari SS, Kant T, Desai YM. Application of polymer composites in civil construction: a general review. Compos Struct 2008;84:114–24.
[5] Nigro E, Cefarelli G, Bilotta A, Manfredi G, Cosenza E. Fire resistance of concrete slabs reinforced with FRP bars. Part I: experimental investigations on the mechanical behavior. Compos Part B Eng 2011;42:1739–50.
[6] Nigro E, Cefarelli G, Bilotta A, Manfredi G, Cosenza E. Fire resistance of concrete slabs reinforced with FRP bars. Part II: experimental results and numerical simulations on the thermal field. Compos Part B Eng 2011;42: 1751–63.
[7] Sadek AW, El-Hawary MM, El-Dieb AS. Fire resistance testing of concrete beams reinforced by GFRP rebars. J Appl Fire Sci 2006;14:91–104.
[8] Carvelli V, Pisani MA, Poggi C. High temperature effects on concrete members reinforced with GFRP rebars. Compos Part B 2013;54:125–32.
[9] Abbasi A, Hogg P. Fire testing of concrete beams with fibre reinforced plastic rebar. Compos Part A 2006;37:1142–50.
[10] Saafi M. Effect of fire on FRP reinforced concrete members. Compos Struct 2002;58:11–20.
[11] McIntyre E, Bisby L, Stratford T. Bond strength of FRP reinforcement in concrete at elevated temperature. In: Proceedings of the 7th International Conference on FRP Composites in Civil Engineering – CICE, Vancouver (Canada); 2014.
[12] Nigro E, Bilotta A, Cefarelli G, Manfredi G, Cosenza E. Performance under fire situations of concrete members reinforced with FRP rods: bond models and design Nomograms. J Compos Constr – ASCE 2012;16:395–406.
[13] Yu B, Kodur V. Factors governing the fire response of concrete beams reinforced with FRP rebars. Compos Struct 2013;100:257–69.
[14] Pagani R, Bocciarelli M, Carvelli V, Pisani M. Modelling high temperature effects on bridge slabs reinforced with GFRP rebars. Eng Struct 2014;81:318–26.
[15] CAN/CSA S806-02 Design and construction of building components with fiber reinforced polymers. Ottawa, ON: Canadian Standards Association; 2002.
[16] Nigro E, Cefarelli G, Bilotta A, Manfredi G, Cosenza E. Guidelines for flexural resistance of FRP reinforced concrete slabs and beams in fire. Compos Part B 2014;58:103–12.
[17] Schmitt A, Pahn M. Examination of the structural behaviour of filigree GFRP-reinforced concrete slabs under bending. In: Improving Performance of Concrete Structures – The Fourth International Fib Congress. Mumbai: Universities Press; 2014. p. 761–3.
[18] Schmitt A, Pahn M. Investigation on flexural stressed sandwich panels with GFRP-reinforcement. In: Proceedings of the 7th International Conference on FRP Composites in Civil Engineering – CICE, Vancouver (Canada); 2014. p. 164–9.
[19] «Schöck ComBAR®» [Online]. Available: http://www.schoeck-combar.com/comb/combar-gfrp-reinforcement/material-138.
[20] «FiReP® Rebar P» [Online]. Available: http://en.firepworld.com/products/firep-rebar.
[21] CEN EN 12390-6:2000. Tensile splitting strength of test specimens. rue de Stassart, 36 B-1050 Brussels, Belgium: European Committee for Standardization, Management Centre; 2000.
[22] ACI 440.1R-06. Guide for the design and construction of structural Concrete reinforced with FRP bars. American Concrete Institute; 2006.